

# Two-step melting in two dimensions: First-order liquid-hexatic transition

Etienne P. Bernard\* and Werner Krauth†

*Laboratoire de Physique Statistique  
Ecole Normale Supérieure, UPMC, CNRS  
24 rue Lhomond, 75231 Paris Cedex 05, France  
(Dated:)*

Melting in two spatial dimensions, as realized in thin films or at interfaces, represents one of the most fascinating phase transitions in nature, but it remains poorly understood. Even for the fundamental hard-disk model, the melting mechanism has not been agreed on after fifty years of studies. A recent Monte Carlo algorithm allows us to thermalize systems large enough to access the thermodynamic regime. We show that melting in hard disks proceeds in two steps with a liquid phase, a hexatic phase, and a solid. The hexatic-solid transition is continuous while, surprisingly, the liquid-hexatic transition is of first-order. This melting scenario solves one of the fundamental statistical-physics models, which is at the root of a large body of theoretical, computational and experimental research.

Generic two-dimensional particle systems cannot crystallize at finite temperature[1–3] because of the importance of fluctuations, yet they may form solids[4]. This paradox has provided the motivation for elucidating the fundamental melting transition in two spatial dimensions. A crystal is characterized by particle positions which fluctuate about the sites of an infinite regular lattice. It has long-range *positional* order. Bond orientations are also the same throughout the lattice. A crystal thus possesses long-range *orientational* order. The positional correlations of a two-dimensional solid decay to zero as a power law at large distances. Because of the absence of a scale, one speaks of “quasi-long range” order. In a two-dimensional solid, the lattice distortions preserve long-range orientational order[5], while in a liquid, both the positional and the orientational correlations decay exponentially.

Besides the solid and the liquid, a third phase, called “hexatic”, has been discussed but never clearly identified in particle systems. The hexatic phase is characterized by exponential positional but quasi-long range orientational correlations. It has long been discussed whether the melting transition follows a one-step first-order scenario between the liquid and the solid (without the hexatic) as in three spatial dimensions[6]), or whether it agrees with the celebrated Kosterlitz, Thouless[7], Halperin, Nelson[8] and Young[9] (KTHNY) two-step scenario with a hexatic phase separated by continuous transitions from the liquid and the solid[10–18].

Two-dimensional melting was discovered [4] in the simplest particle system, the hard-disk model. Hard disks (of radius  $\sigma$ ) are structureless and all configurations of non-overlapping disks have zero potential energy. Two isolated disks only feel the hard-core repulsion, but the other disks mediate an entropic “depletion” interaction (see, e.g., [19]). Phase transitions result from an “order from disorder” phenomenon: At high density, ordered configurations can allow for larger local fluctuations, thus higher entropy, than the disordered liquid. For hard disks, no

difference exists between the liquid and the gas. At fixed density  $\eta$ , the phase diagram is independent of temperature  $T = 1/k_B\beta$ , and the pressure is proportional to  $T$ , as discovered by D. Bernoulli in 1738. Even for this basic model, the nature of the melting transition has not been agreed on.

The hard-disk model has been simulated with the local Monte Carlo algorithm since the original work by Metropolis et al. [20]. A faster collective-move “event-chain” Monte Carlo algorithm was developed only recently[21] (see [22]). We will use it to show that the melting transition neither follows the one-step first-order nor the two-step continuous KTHNY scenario.

To quantify orientational order, we express the local orientation of disk  $k$  through the complex vector  $\Psi_k = \langle \exp(6i\phi_{kl}) \rangle$ , with  $\langle \rangle$  the average over all the neighbors  $l$  of  $k$ . The angle  $\phi_{kl}$  describes the orientation of the bond  $kl$  with respect to a fixed axis. The sample orientation is defined as  $\Psi = 1/N \sum_k \Psi_k$ . For a perfect triangular lattice, all the angles  $6\phi_{kl}$  are the same and  $|\Psi_k| = |\Psi| = 1$  (see [22]).

In Fig. 1, the local orientations of a configuration with  $N = 1024^2$  disks at density  $\eta = N\pi\sigma^2/V = 0.708$  in a square box of volume  $V$  are projected onto the sample orientation and represented using a color code (see [22]). Inside this configuration, a vertical stripe with density  $\sim 0.716$  preserving orientational order over long distances coexists with a stripe of disordered liquid of lower density  $\sim 0.700$ . Each stripe corresponds to a different phase. The two interfaces of length  $\simeq \sqrt{N}$  close on themselves *via* the periodic boundary conditions. Stripe-shaped phases as in Fig. 1a are found in the center of a coexistence interval  $\eta \in [0.700, 0.716]$ , whereas close to its endpoints, a “bubble” of the minority phase is present inside the majority phase for  $\eta \gtrsim 0.700$  and  $\eta \lesssim 0.716$  (see Fig. 2). This phase coexistence is the hallmark of a first-order transition.

The first-order transition shows up in the equilibrium equation of state  $P(V)$  (see Fig. 2). At finite  $N$ ,

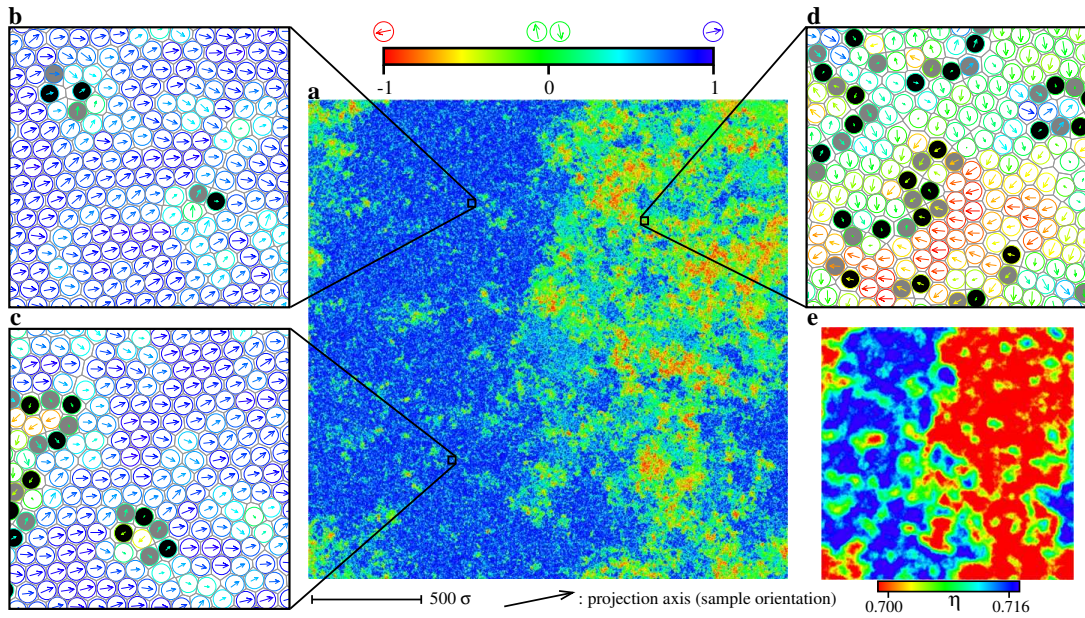


FIG. 1. Phase-coexistence for  $1024^2$  thermalized hard disks at density  $\eta = 0.708$ . **a**: Color-coded local orientations  $\Psi_k$  showing long orientational correlations (blue region, see **b,c**) coexisting with short-range correlations (see **d**). **e**: Local densities (averaged over a radius of  $50\sigma$ ), demonstrating the connection between density and local orientation (see [22]). In **b, c, d**, disks with five (seven) neighbors are colored in gray (black).

the free energy is not necessarily convex (as it would be in an infinite system) and the equilibrium pressure  $P(V) = -\partial F/\partial V$  can form a thermodynamically stable loop due to the interface free energy. The pressure loop in the coexistence window of a finite system is caused by the curved interface between a bubble of minority phase and the surrounding majority phase (see Fig. 2**b,d**). In a system with periodic boundary conditions, the pressure loop contains a horizontal piece corresponding to the “stripe” regime, where the interfaces are flat. This is visible near  $\eta \sim 0.708$  for the largest systems in Fig. 2. In a finite system, the Maxwell construction suppresses the interface effects. For the equation of state of Fig. 2**a**, this construction confirms the boundary densities  $\eta = 0.700$  and  $\eta = 0.716$  of Fig. 1 for the coexistence interval, with very small finite-size effects. The interface free energy per disk, the hatched area in Fig. 2, depends on the length  $\propto \sqrt{N}$  of the interface in the “stripe” regime so that  $\Delta f = \Delta F/N \propto 1/\sqrt{N}$  (see Fig. 2**f**).

The first-order nature of the transition involving the liquid is thus established by *i*): The visual evidence of phase coexistence in Fig. 1, *ii*): The  $\propto 1/\sqrt{N}$  scaling of the interface free energy per disk[23], and *iii*): The characteristic shape of the equation of state in a finite periodic system [24–26]. We stress that the system size is larger than the physical length scales so that the results hold in the thermodynamic limit (see [22]).

In the coexistence interval, the individual phases are difficult to analyze at large length scales because of the fluctuating interface, and only the low-density coexisting

phase is identified as a liquid with orientational correlations below a scale of  $\sim 100\sigma$  (see Fig. 1**a,d**). Unlike constant  $NV$  simulations, Gibbs ensemble simulations can have phase coexistence without interfaces, but these simulations are very slow at large  $N$  (see [22]). The single-phase system at density  $\eta = 0.718$ , is above the coexistence window for all  $N$  (see Fig. 2), and it allows us to characterize the high-density coexisting phase.

Positional order can be studied in the two-dimensional pair correlation  $g(\Delta\mathbf{r})$ , the high-resolution histogram of periodic pair distances  $\Delta\mathbf{r}_{ij} = \mathbf{r}_i - \mathbf{r}_j$  sampled from all  $N(N-1)/2$  pairs  $i, j$  of disks. To average this two-dimensional histogram over configurations (as in Fig. 3) the latter are oriented such that the  $\Delta x$  axis points in the direction of the sample orientation  $\Psi$ . At short distances, hexagonal order is evident at  $\eta = 0.718$  (see Fig. 3**a**). The excellent contrast between peaks and valleys of  $g(\Delta\mathbf{r})$  at small  $|\Delta\mathbf{r}| \gtrsim 2\sigma$  underlines the single-phase nature of the system at this density. The cut of the histogram along the positive  $\Delta x$  axis leaves no doubt that the system has exponentially decaying positional order on a length scale of  $\sim 100\sigma$  and cannot be a solid. The (one-dimensional) positional correlation function  $c_{\mathbf{k}}(r)$ , computed by Fourier transform of  $g(\Delta\mathbf{r})$ , fully confirms these statements (see [22]).

The orientational correlations at density  $\eta = 0.718$  decay extremely slowly and do not allow us to distinguish between quasi-long range and long-range order (see [22]). However, short-ranged positional correlation is inconsistent with long-ranged orientational order. It follows that

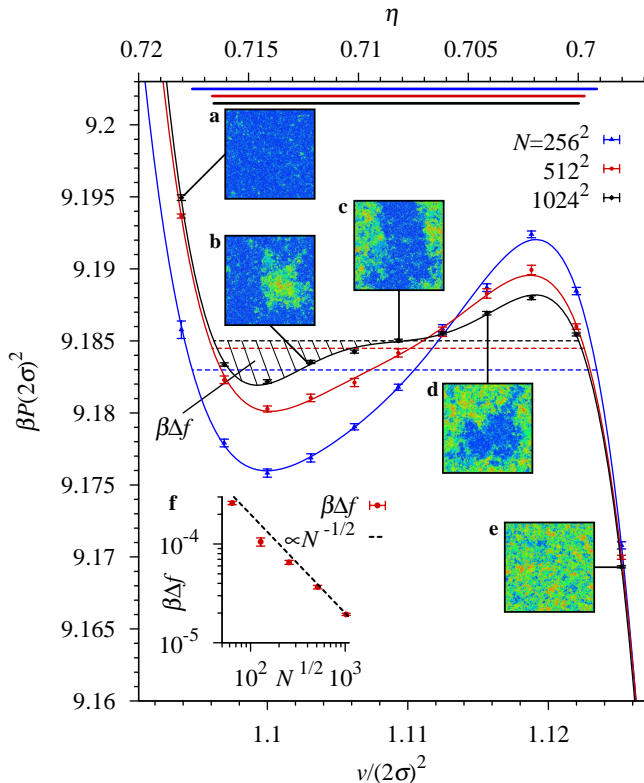


FIG. 2. Equilibrium equation of state for hard disks. The pressure is plotted *vs.* volume per particle ( $v = V/N$ ) (lower scale) and density  $\eta$  (upper scale). In the coexistence region, the strong system-size dependence stems from the interface free energy. The Maxwell constructions (horizontal lines) suppress the interface effects (with a convex free energy) for each  $N$ . “Stripe” (c, for  $N = 1024^2$ ) and “bubble” configurations (b,d) are shown in the coexistence region, together with two single-phase configurations (a,e). The interface free energy per disk  $\beta\Delta f$  (hatched area) scales as  $1/\sqrt{N}$  (f).

the orientation must be quasi-long ranged with a small exponent  $\lesssim 0$ , and that the system at  $\eta = 0.718$  and the high-density coexisting phase are both hexatic.

The two-dimensional pair correlation  $g(\Delta\mathbf{r}) - 1$  of Fig. 3b allows us to follow the transition from the hexatic to the solid: The positional order increases continuously with density and crosses over into power-law behavior at density  $\eta \sim 0.720$ , with an exponent  $\simeq -1/3$  which corresponds to the stability limit of the solid phase in the KTHNY scenario. The hexatic-solid transition thus takes place at  $\eta \gtrsim 0.720$ . At this density, the positional correlation function at large distances  $r$ , displays the finite-size effects characteristic of a continuous transition, but up to a few hundred  $\sigma$ ,  $c_k$  is well stabilized with system size (see [22]). Moreover, no pressure loop is observed in the equation of state, and the compressibility remains very small. The system is clearly in a single phase. Unlike the liquid-hexatic transition, the hexatic-solid transition therefore follows the KTHNY scenario, and is continu-

ous.

The single-phase hexatic regime is confined to a density interval  $\eta \in [0.716, 0.720]$ . Although narrow, it is an order of magnitude larger than the scale set by density fluctuations for our largest systems and can be easily resolved (see [22]). In the hexatic phase, the orientational correlations decay extremely slowly. The exponent of the orientational correlations is close to zero and negative. It remains far from the lower limit of  $-1/4$  at the continuous KTHNY transition, as this transition is preempted by a first-order instability.

The event-chain algorithm is about two orders of magnitude faster than the local Monte Carlo used up to now, allowing us to thermalize for the first time dense systems with up to  $1024^2$  disks. To illustrate convergence toward thermal equilibrium and to check that hard disks in the window of densities  $\eta \in [0.700, 0.716]$  are indeed phase-separated, we show in Fig. 4 two one-week simulations of our largest systems after quenches from radically different initial conditions, namely the (unstable) crystal, with  $|\Psi| = 1$ , and the liquid, for which  $|\Psi| \simeq 0$ . For both initial conditions, a slow process of coarsening takes place (see Fig. 4a,b). Phase separation is observed after  $\sim 10^6$  displacements per disk, and the sample orientation takes on similar absolute values (see Fig. 4c). Effective simulation times of many earlier calculations were much shorter[14, 15], and the simulations remained in an out-of-equilibrium state which is homogeneous on large length scales, whereas the thermalized system is phase-separated and therefore inhomogeneous. The production runs for  $N = 1024^2$  were obtained from Markov chains with running times of nine months, 30 times larger than those of Fig. 4a,b.

The solution of the melting problem presented in this work provides the starting point for the understanding of melting in films, suspensions, and other soft-condensed-matter systems. The insights obtained combine thermodynamic reasoning with powerful tools: advanced simulation algorithms, direct visualization, and a failsafe analysis of correlations. These tools will all be widely applicable, for example to study the cross-over from two to three-dimensional melting as it is realized experimentally with spheres under different confinement conditions[17].

In simple systems such as hard disks and spheres, entropic and elastic effects have the same origin: elastic forces are entropically induced. For general interaction potentials, entropy and elasticity are no longer strictly linked and order-disorder transitions, which can then take place as a function of temperature or of density, might realize other melting scenarios[27]. Theoretical, computational and experimental research on more complex microscopic models will build on the hard-disk solution obtained in this work.

We are indebted to K. Binder and D. R. Nelson for helpful discussions and correspondence. We thank J. Dalibard and G. Bastard for a critical reading of the



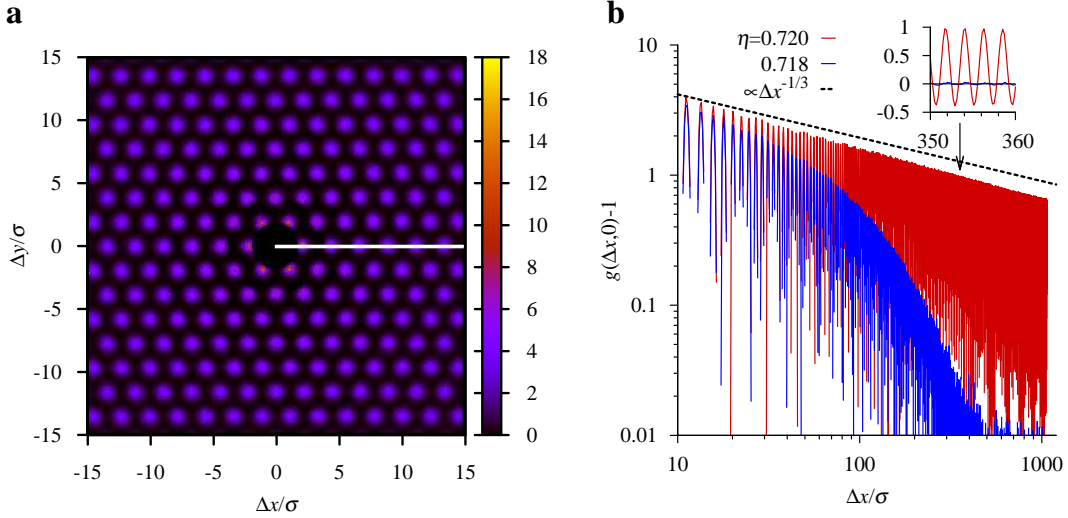


FIG. 3. Configuration-averaged two-dimensional pair correlation.  $g(\Delta\mathbf{r})$  is obtained from the two-dimensional histogram of periodic distances  $\Delta\mathbf{r}_{ij} = \mathbf{r}_i - \mathbf{r}_j$ . **a**: Pair correlation  $g(\Delta\mathbf{r})$  at density  $\eta = 0.718$  for small  $\Delta\mathbf{r} = (\Delta x, \Delta y)$ . Each disk configuration is oriented with respect to  $\Psi$ . The excellent contrast between the peak and the bottom values of  $g(\Delta\mathbf{r})$  at  $|\Delta\mathbf{r}| \gtrsim 2\sigma$ , of about (16 : 0.2), provides evidence for the single-phase nature of the system. **b**: Cut of the sample-averaged  $g(\Delta\mathbf{r}) - 1$  for  $\Delta\mathbf{r} = (\Delta x, 0)$ . Decay is exponential for  $\eta = 0.718$  and algebraic for  $\eta = 0.720$ . (See [22] for positional and orientational correlation functions.)

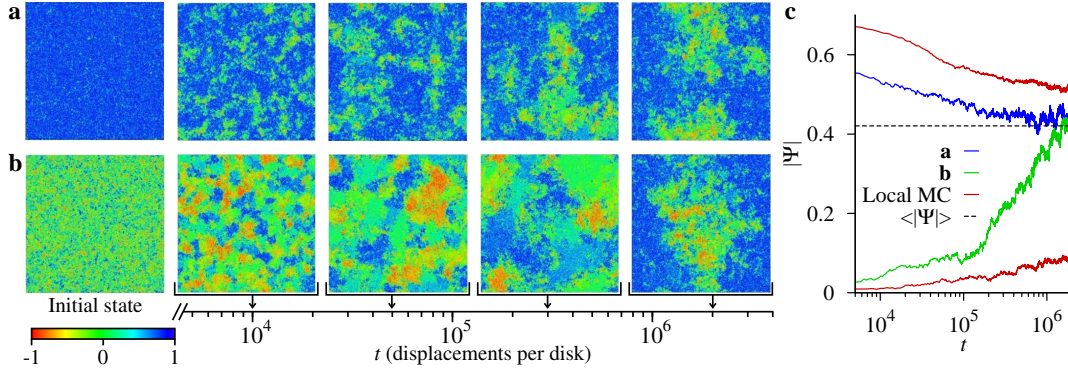


FIG. 4. Approach to thermal equilibrium from different initial conditions. **a,b**:  $1024^2$  hard disks at density  $\eta = 0.708$ , after a quench from a high-density crystal (**a**) and from a low-density liquid (**b**), showing coarsening leading to phase separation (Color code for  $\Psi_k$  as in Fig. 1b, see also [22]). Each of the runs takes about one week of CPU time. **c**: Absolute value of the sample orientation for the simulations in **a,b**, compared to runs with the local Monte Carlo algorithm from the same initial conditions (time in attempted displacements per disk). The correlation time of the event-chain algorithm, on the order of  $10^6$  displacements per disk, estimated from **c**, agrees with the correlation time estimated in our production runs with  $6 \times 10^7$  total displacements per disk.

manuscript.

\* etienne.bernard@lps.ens.fr

† werner.krauth@ens.fr

[1] R. Peierls, *Helv. Phys. Acta Suppl.* 7, 81 (1934)

[2] R. Peierls, *Annales de l'IHP* 5 177 (1935)

[3] N. D. Mermin, H. Wagner, *Phys. Rev. Lett.* 17, 1133 (1966).

[4] B. J. Alder, T. E. Wainwright, *Phys. Rev.* 127, 359 (1962)

[5] N. D. Mermin, *Phys. Rev.* 176, 250 (1968)

[6] W. G. Hoover, F. H. Ree, *J. Chem. Phys.* 49, 3609 (1968).

[7] J. M. Kosterlitz, D. J. Thouless, *J. Phys. C* 6, 1181 (1973).

[8] B. I. Halperin, D. R. Nelson, *Phys. Rev. Lett.* 41, 121 (1978).

[9] A. P. Young, *Phys. Rev. B* 19, 1855 (1979).

[10] K. J. Strandburg, *Rev. Mod. Phys.* 60, 161 (1988).

[11] J. Y. Lee, K. J. Strandburg, *Phys. Rev. B* 46, 11190 (1992).

[12] J. A. Zollweg, G. V. Chester, *Phys. Rev. B* 46, 11186 (1992).

- [13] H. Weber, D. Marx, K. Binder, *Phys. Rev. B* 51 14636 (1995).
- [14] A. Jaster, *Phys. Lett. A* 330, 120 (2004).
- [15] C. H. Mak, *Phys. Rev. E* 73, 065104(R) (2006).
- [16] K. Zahn, R. Lenke, G. Maret, *Phys. Rev. Lett.* 82, 2721 (1999).
- [17] Y. Peng, Z. Wang Z., A. M. Alsayed, A. G. Yodh, Y. Han, *Phys. Rev. Lett.* 104, 205703 (2010).
- [18] K. Bagchi, H. C. Andersen, W. Swope, *Phys. Rev. Lett.* 76 255 (1996).
- [19] W. Krauth, *Statistical Mechanics: Algorithms and Computations*. Oxford University Press (2006)
- [20] N. Metropolis, A. W. Rosenbluth, M. N. Rosenbluth, A. H. Teller, E. Teller, *J. Chem. Phys.* 21 1087 (1953).
- [21] E. P. Bernard, W. Krauth, D. B. Wilson, *Phys. Rev. E* 80 056704 (2009).
- [22] See Supplemental Material at [URL will be inserted by publisher].
- [23] J. Lee, J. M. Kosterlitz, *Phys. Rev. Lett.* 65, 137 (1990).
- [24] J. E. Mayer, W. W. Wood, *J. Chem. Phys.* 42, 4268 (1965)
- [25] H. Furukawa, K. Binder, *Phys. Rev A* 26, 556 (1982)
- [26] M. Schrader, P. Virnau, K. Binder, *Phys Rev E* 79, 061104 (2009)
- [27] A. C. D. van Enter, S. B. Shlosman, *Phys. Rev. Lett.* 89 285702 (2002).